Journal Pre-proof

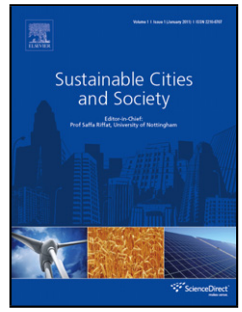

Techno-economic analysis of grid-integrated PV/wind systems for electricity reliability enhancement in Ethiopian industrial park

Tefera Mekonnen Azerefegn, Ramchandra Bhandari, A. Venkata Ramayya

PII: S2210-6707(19)31418-0

DOI: https://doi.org/10.1016/j.scs.2019.101915

Reference: SCS 101915

To appear in: *Sustainable Cities and Society*

Received Date: 21 May 2019

Revised Date: 25 October 2019

Accepted Date: 25 October 2019

Please cite this article as: Azerefegn TM, Bhandari R, Ramayya AV, Techno-economic analysis of grid-integrated PV/wind systems for electricity reliability enhancement in Ethiopian industrial park, *Sustainable Cities and Society* (2019), doi: https://doi.org/10.1016/j.scs.2019.101915

Techno-economic analysis of grid-integrated PV/wind systems for electricity reliability enhancement in Ethiopian industrial park

Tefera Mekonnen Azerefegn[a] *, Ramchandra Bhandari [a], A.Venkata Ramayya[b]

[a] Institute for Technology and Resources Management in the Tropics and Subtropics (ITT), TH Köln (University of Applied Science), Betzdorfer Strasse 2, 50679 Cologne, Germany

[b] Jimma University, Institute of Technology, Jimma, Ethiopia

*Corresponding author: Email: mtefee@gmail.com; Tel.: +491632035866

The authors would like to thank Ethiopian National Meteorology Agency and Ethiopian Electric Utility for their cooperation to provide the meteorological, load, and grid data. The authors are also thankful to the National Renewable Energy Laboratories (NREL) for providing the HOMER Pro software free. Last but not least, our exceptional thanks go to Ethiopian Ministry of Science and Higher Education and the German Development Bank (KfW) through ExiST project for funding this research.

Highlights

- The techno-economic feasibility analysis of grid-tied PV/wind power systems are investigated under unscheduled **grid outage** consideration.
- Three different climate regions of industrial park load is considered and analyzed
- Four main operational scenarios are developed, and optimal system configuration is achieved.
- The grid/diesel/PV/battery systems are the best supply option for all three regions among the considered scenarios.
- Sensitivity analyses have been performed on the optimized grid/diesel/PV/battery systems in order to observe the future performance of the systems.

Abstract

In most developing countries, the electricity supply system is highly unreliable. Ethiopia is one of the least developed country in the world, and the existing distribution system of the country has encountered frequent power interruptions. During this interruption, diesel generator supplied the critical load of most industries in the country. This paper examines the feasibility of integrating PV/wind power systems into existing unreliable grid/diesel generator systems for supplying the critical loads of industrial parks in three different regions of Ethiopia. The study focused on how to provide a reliable supply with cost-effective and environment-friendly resources. Based on load variation, grid interruption, and meteorological data of the study areas, modeling and techno-economic analysis of grid-connected PV/wind/diesel systems were carried out using HOMER Pro software by exploring four different scenarios involving the consideration of unscheduled outages. Results showed that grid//diesel/PV/battery systems are technically, economically, and environmentally feasible for all three climate regions with the cost of energy at 0.044, 0.049, and 0.048 $/kWh, respectively. Also found that excess electricity, cost of energy, and the net present cost is slightly increased with PV penetration, whereas the CO_2 emissions for these locations decreased by 45%, 44%, and 42% compared to the existing systems.

Keywords: Unreliable grid, Grid-connected systems, PV, Wind, Industrial park, Techno-economic analysis.

Nomenclature

COE	Cost of energy	i	The annual real interest rate (%),
CRF	Capital recovery factor	i_n	The nominal interest rate (%)
CHP	Combined heat and power	*N*	The lifetime of the project (year)

DG	Distributed generation	n_{bb}	The battery charging efficiency
EEU	Ethiopian electric utility	n_{bi}	The inverter efficiency
GTP	Growth and transformation plan	P_{gen}	The electrical output of the generator
HOMER	Hybrid optimization model for electric renewables	P_{pv}	The average power output of the PV array
IP	Industrial park	S	Monthly average daily number of hours of bright sunshine
NASA	National aeronautics and space administration	S_O	Maximum possible daily bright sunshine hour
NPC	Net present cost	T_C	The PV cell temperature in the current time step (°C)
NMA	National meteorology agency	$T_{c.STC}$	The PV cell temperature under standard test (25 °C)
PV	photovoltaic	$v(z)$	Wind speed at height of Z m above ground (m/s)
RF	Renewable fraction	V_r	wind speed at reference height (m/s)
SNNP	Southern nation nationalities and people	$Ygen$	The rated capacity of the generator (kW)
Cp	The power coefficient.	Y_{pv}	The peak power output of PV
C_T	The total annualized cost ($/year)	Z	Elevation above ground (m)
Eb	The battery energy in time interval	Z_0	Surface roughness length (m)
E_{gs}	Energy sold to the grid per year (kWh/yr)	Z_r	Reference height (m)
F_1	The fuel curve slope in (L/hr/kW_{output})	A_T	the swept area (m^2)
f	Inflation rate (%).	α_p	The temperature coefficient of PV (%/°C)
F	Fuel consumption rate (L/hour)	σ	The self-discharging factor
F_0	Generator fuel curve intercept coefficient	ρ	Air density (kg/m^3)
f_{pv}	The PV derating factor	δ	Declination angle (^{0})
G_{SC}	The solar constant = 1367 (W/m^2)	ϕ	Latitude angle (^{0})
G_T	The solar radiation incident on the PV array in the current time step (kW/m^2)	ω_s	The sunset hour angle (^{0})
$G_{T.STC}$	The incident radiation at standard test conditions ($1kW/m^2$)		
H	Monthly average daily radiation on a horizontal surface		
H_O	Monthly average daily extraterrestrial radiation on a horizontal surface (MJ/m^2)		

1. Introduction

Ethiopia is well endowed with various renewable energy resources, and has a potential to generate more than 60,000 megawatts of electric power from hydro, solar, wind, and geothermal sources [1,2]. Currently, the country has approximately 4284 MW of installed generation capacity to serve a population of about 105 million people [2,3]. From the entire installed capacity, 89% of electricity is generated from hydropower [4].

Even though the country has significant electricity generating potential, it is still characterized by being one of the least electrified countries of the world with frequent and prolonged grid outages. According to a report [5], in Ethiopia, there are 8.2 electrical outages in a typical month with an average outage duration lasting 5.8 hours. All industrial, commercial and residential customers can be affected by this outage. Especially for industries, it is challenging to tolerate outages, since it causes much revenue loss within half an hour of interruption.

To mitigate the negative impact of grid outage on the customer, in many locations around the globe, on-grid site was equipped with a diesel generator as a backup power source [6]. The majority of the industry zones in Ethiopia also use diesel generators as a backup [7]. However, the combustion of diesel for power generation can produce undesirable gasses, like carbon dioxide (CO_2), carbon monoxide (CO) nitrogen oxides (NO_x), sulfur dioxide (SO_2), and particulate matter (PM) [8]. These gasses have a detrimental impact on the environment and future human life [9,10]

Based on the continuing commercial maturation of distributed generation (DG) technologies like PV and wind turbines, the addition of these renewable energy sources into diesel generator alleviates environmental concern and fuel price uncertainties [11,12]. Ethiopia has also a target to reach a share of 15-20 % of its energy supply from non-hydropower-based renewable resources (solar, wind, and geothermal) by 2020 to realize a zero net carbon emission up to 2025 [13,14]. Consequently, the government of Ethiopia is motivating on the exploration of renewable distributed generation technologies.

To achieve the targeted goals of the country, analyzing grid-connected solar/wind power systems could be one of the viable options. Such kind of grid-tied renewable distributed generation systems not only offer environmental benefit and electric service, but also provides customer benefits through selling excess power generated by the systems to the grid [15,16].Various studies have analyzed the techno-economic feasibility of grid-integrated renewable distributed generation systems using different optimization techniques.

Islam [17] presented the techno-economic analysis of grid-tied PV/hydropower systems for a huge office building in the southeastern part of France using HOMER software. Results showed that PV/grid systems were more cost effective than grid-only systems. In Ref. [18], the economic and technical analysis of grid-connected PV systems at different sites of Saud Arabia was explored using RETScreen simulation tool. The results indicated that from selected site Bisha was the best area for the implementation of grid-connected solar PV systems. Gonzalez et al. [19] discussed the economic and environmental impact of grid-connected PV/wind/biomass systems in central Catalonia using genetic algorithm optimization technique. Results showed that the grid-integrated hybrid renewable systems were less cost-effective than the grid-only systems, but it has lower environmental impacts compared to grid-only systems. Li et al. [20] evaluated the techno-economic performance of grid-connected PV systems in the five climate zones of China using HOMER software. The results indicated that grid/PV systems were technically and economically feasible for all five climate zones. Kazem et al. [21] studied the techno-economic viability of 1MW PV grid-connected systems in Oman with the help of numerical simulation using MATLAB developed code. They found that the proposed grid-integrated PV systems were economically feasible. Bastholm and Fiedler [22] evaluated the techno-economic analysis of grid-connected PV/diesel/battery power systems under national grid blackouts in Tanzania using HOMER simulation tools. From the result, they found that for power outages above 0.75 hour per day, grid-tied PV/diesel/battery systems were economically feasible for the considered load in the locations. Algarni et al. [23] analyzed grid-tied PV systems under different tracking condition in Makkah, Saudi Arabia using HOMER simulation software. The results suggested that grid-connected vertical axis tracker was more cost effective than horizontal axis tracker for the considered location. Rehman et al. [24] analyzed grid-connected PV systems for household in Pakistan under grid outage consideration using HOMER Pro simulation tool. The results pointed that grid-tied PV systems with battery storage were both economically and technically viable for the case under consideration. Jahangiri et al. [25] evaluated the techno- economic and environmental analysis of grid/wind/ PV systems for the provision of electricity and hydrogen in the southern location of Iran using HOMER Pro software. The results depicted that grid/wind/PV systems were the most optimal mode for electricity generation with COE 1.55$/kWh, and 0.496 $ per kg of hydrogen generation price was achieved using the main grid only. Mukisa et al.[26] studied the feasibility assessment of grid-integrated rooftop solar photovoltaic systems for 36 industrial application in Uganda. Google Earth and Azimuth tools were used to determine the rooftop area. The results showed that the proposed PV systems were economically viable.

Other studies have also addressed the techno-economic analysis of off-grid hybrid power systems in the combination of PV/wind/battery [27–30], PV/diesel/battery [31–33] PV/wind/battery/diesel [34–39] PV/fuel cell/diesel [40] and PV/wind/diesel systems [41,42] in different locations.

As it is mentioned in the above literature, the techno-economic analysis of off-grid and grid-connected hybrid renewable systems have been investigated in several studies. However, the techno-economic comparative study of grid-connected renewable DG by considering the effect of an outage is not explored thoroughly enough. Notably, the effect of unscheduled outages has so far not been considered in sufficient detail. Therefore, the main focus of this study is to examine the techno-economic performance of grid-connected PV/wind power systems under unscheduled grid outage consideration for the industrial park (IP) load, in three different regions of Ethiopia. Previously diesel generator was used as a backup to support the unreliable hydro-based grid power of the IP. In this regard, this study also investigated the means to reduce the consumption of diesel fuel and the working hours of diesel generators. The performance of the designed system is simulated using the HOMER Pro optimization software [43,44].

The rest of the paper is structured as follows: Section 2 presents the site description of the study regions. Methodology and modeling of grid-connected PV/wind power systems of the locations are introduced in section 3. Simulation results and discussions are provided in section 4. Finally, the conclusions of this study are described in section 5.

2. Background Information

2.1. Site background

The second Growth and Transformation Plan (GTP II) of Ethiopia was endorsed by the council of ministers to guide development endeavors within the country under the implementation for 2015-2020 [45]. Development and expansion of industrial parks are one of the sectors to which GTP

II gave attention, and based on the plan several industrial parks are being developed throughout the country [46,47]. However, due to the high power demand and the climatic impacts on the hydropower system, the industrial park has been facing some power outages that affect the manufacturing process.

Hawassa IP, Kombolcha IP, and Adama IP were the three main industrial parks in the country, and currently unscheduled grid outages shown in Table 2 are considered. To analyze the potential of renewable energy (solar/wind) and to design a reliable supply, these three region's representative parks were also chosen under this study. The geographical layout, overview, and coordinates of the locations are shown in Fig.1 and Table1, respectively.

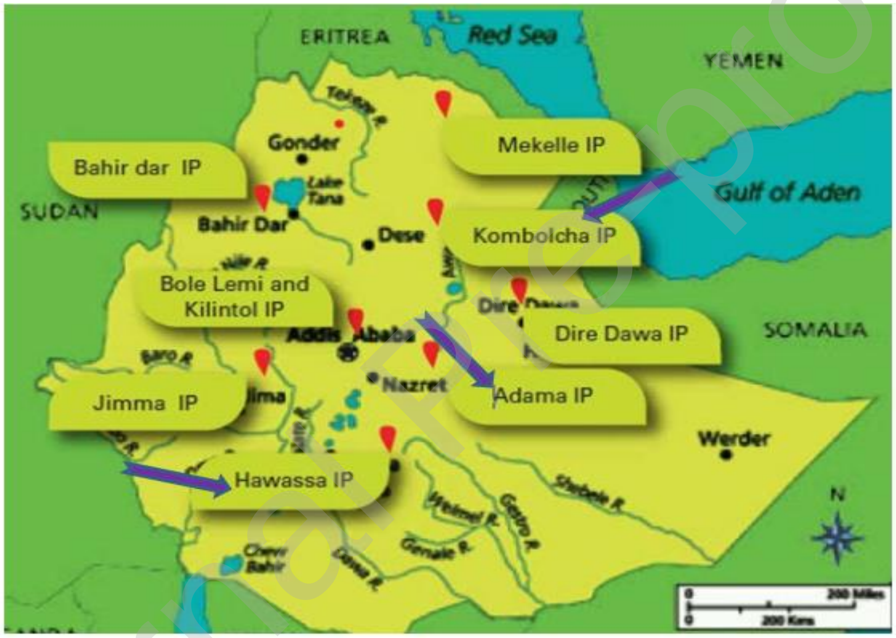

Fig.1. Geographical layout of the project area [[48] , Google Map 2018 edited].

Table1: Overview and geographical coordinate of the study region [46,49–51].

Name of the IP	Region	Latitude (ºN)	Longitude (ºE)	Elevation (m)	Climate regions	Land size of the park in hectare	production	Incoming Voltage to IP substation
Hawassa IP	SNNP	7.06	38.45	1,694	Tropical rainy climate (Savanna)	300	Garment	132kV
Kombolcha IP	Amhara	11.08	39.73	1,857	Warm temper-ature rainy climate	700	Garment and Food	132kV
Adama IP	Oromia	8.54	39.26	1,622	Tropical rainy climate	2,000	Textile and Food	132kV

3. Methodology

The feasibility, techno-economic, optimization, and sensitivity analysis of the grid-connected PV/wind power systems for the selected locations are carried out using HOMER Pro, with the climate, load, grid outage, and economic data as inputs as shown in Fig.2 below.

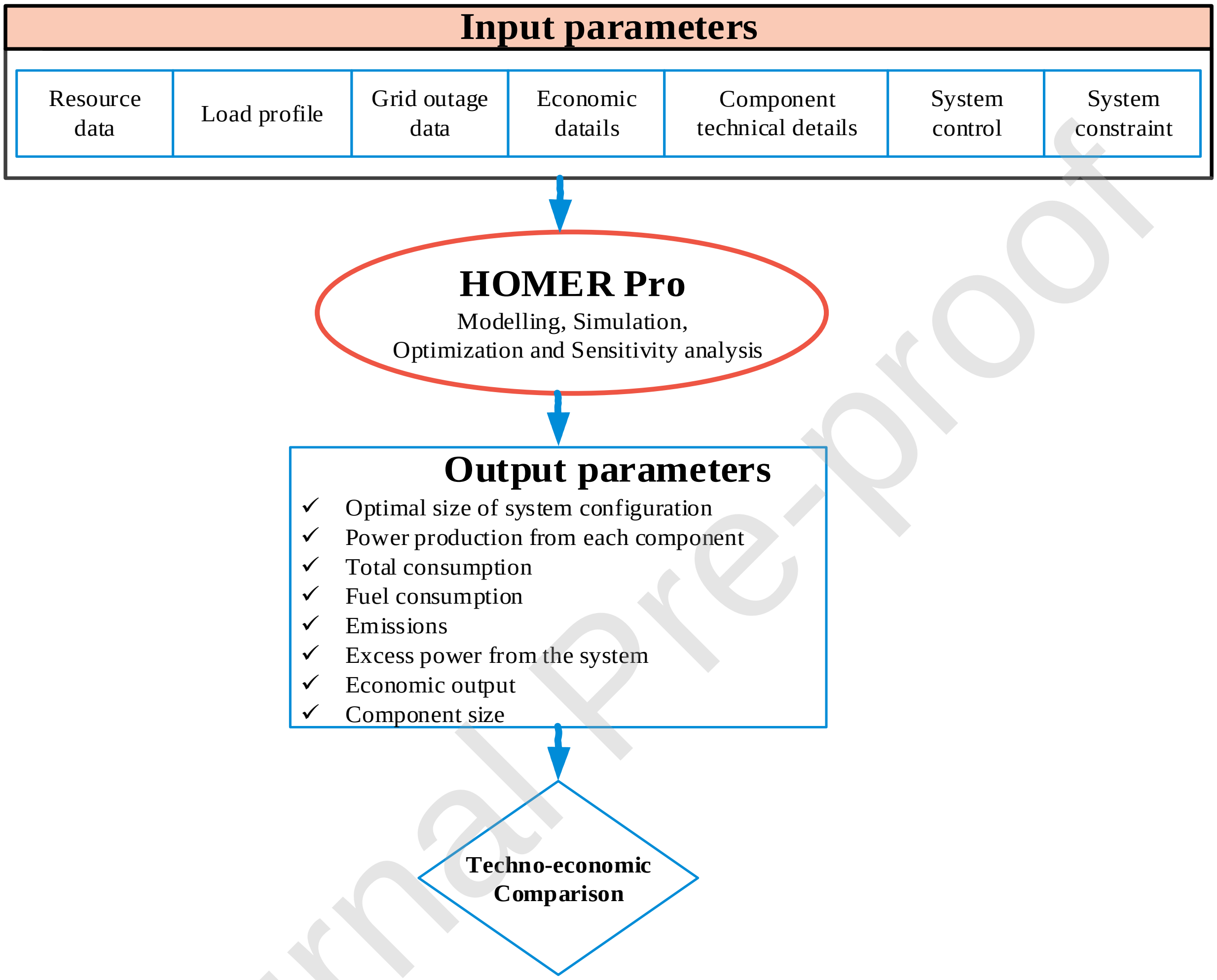

Fig.2. Methodological steps for the study.

3.1. Resource Assessment

In the following subsection, the solar radiation potential and wind resources of the locations are analyzed.

3.1.1. Solar irradiation

For many developing countries including the investigated sites, there is no properly recorded solar radiation data. What usually available is sunshine duration data. However, it is possible to compute the average monthly solar radiation data using empirical Eq. (1) [52–54].

$$H = H_O\left(a + b\left(\frac{S}{S_O}\right)\right) \tag{1}$$

Where H is the monthly average daily radiation on a horizontal surface (MJ$/m^2$), H_O is the monthly average daily extraterrestrial radiation on a horizontal surface (MJ$/m^2$), S is the monthly average daily number of bright sunshine hours, and S_O is the maximum possible daily hours of bright sunshine. Coefficients a and b are regression coefficients based on the coordinates of a location. In this study, the regression coefficients having average values of a = 0.33 and b = 0.43 were used [52]. The Monthly average extraterrestrial radiation is computed using Eq. (2).

$$H_O = \frac{24*3600*G_{SC}}{\pi}\left(1 + 0.033 * cos\left(\frac{360n_d}{365}\right)\right) * \left(cos\phi\, cos\delta\, sin\omega_s + \frac{\pi\omega_s}{180} sin\phi sin\delta\right) \tag{2}$$

Where n_d is the day number starting from January 1st as 1, G_{SC} is the solar constant (1367 W$/m^2$), ϕ is the latitude of the location (7° 04' 0.66''N), δ is the declination angle (^{0}), given by Eq. (3) , and ω_s is the sunset hour angle (^{0}), which is given by Eq (4) below.

$$\delta = 23.45 sin\left(360\frac{284+n_d}{365}\right) \tag{3}$$

$$\omega_s = cos^{-1}(-tan\phi\, tan\delta) \tag{4}$$

The maximum possible sunshine duration S_O is given by;

$$S_O = \frac{2}{15} cos^{-1}(-tan\phi\, tan\delta) \tag{5}$$

Based on the above equations, solar radiation data of the locations were calculated. The computed annual average solar radiation for Hawassa IP, Kombolcha IP, and Adama IP were 6.18 kWh/m^2/day, 5.96 kWh/m^2/day and 6.20 kWh/m^2/day respectively. The yearly average solar radiation of Hawassa IP and Adama IP is nearly the same because both of them are located in the same climate zone. Because of warm temperature and rainy climate nature, the average annual radiation of Kombolcha IP is slightly lower than that of the two sites.

NASA database [55] was additionally used to validate the calculated result. The annual average radiation data taken from NASA for Hawassa IP, Kombolcha IP, and Adama IP were 6.07 kWh/m^2/day, 5.87 kWh/m^2/day, and 6.15 kWh/m^2/day respectively. The monthly calculated solar radiation data and the data obtained from NASA for each region are shown in Fig.3, Fig.4, and Fig.5. For this investigation, the calculated data is considered.

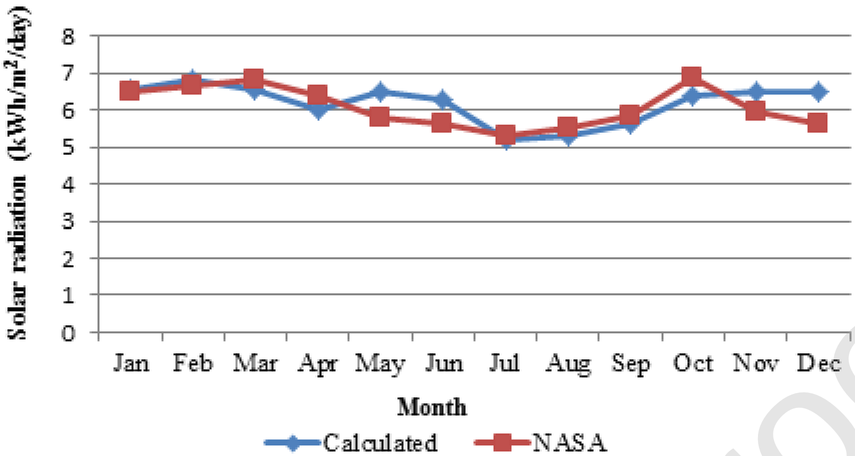

Fig.3. Monthly average calculated and NASA solar radiation data for Hawassa IP.

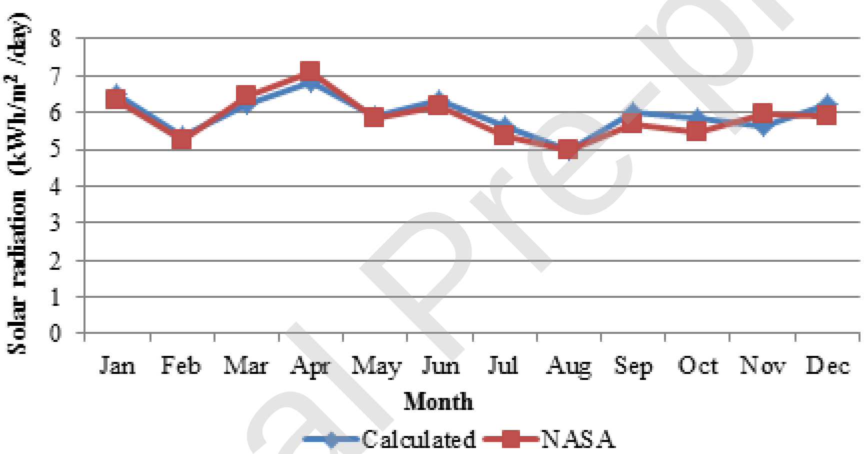

Fig.4. Monthly average calculated and NASA solar radiation data for Kombolcha IP.

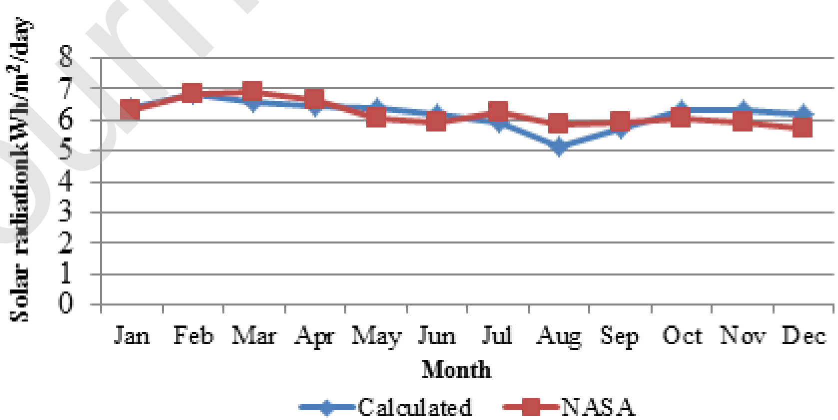

Fig.5. Monthly average calculated and NASA solar radiation data for Adama IP.

In order to determine the actual output power from solar PV, knowing the ambient temperature of the sites is very important. Fig.6 below shows the average monthly temperature of the sites taken from the National Meteorology Agency (NMA) of Ethiopia. The annual average temperatures in Hawassa IP, Kombolcha IP, and Adama IP were 27.9 ^{0}C, 27 ^{0}C, and 28.14 ^{0}C, respectively.

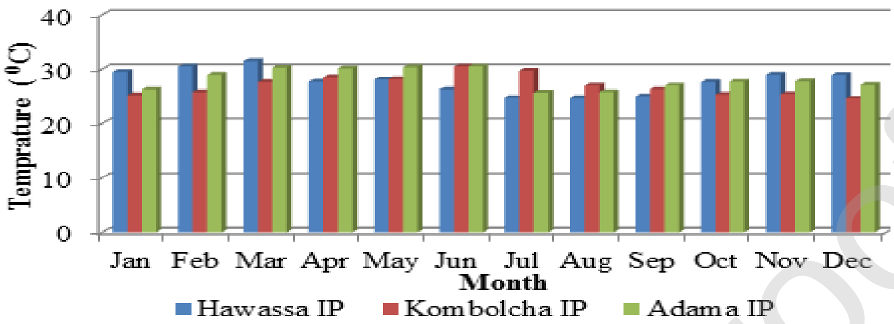

Fig.6. Monthly average ambient temperature data for the study sites.

3.1.2. Wind resource assessment

Wind speed data of the locations were obtained from National Meteorological Agency (NMA). The NMA collects wind speed data at 2 m height, which is below the reference standard of 10 m height placed by the World Meteorological Organization (WMO). However, if the wind speed measurement was not made at the reference height, it is possible to extrapolate to the selected wind turbine hub height using Eq.(6) [56,57].

$$V(z)\ln\left(\frac{Zr}{Zo}\right) = V(Zr)ln\left(\frac{Z}{Zo}\right) \tag{6}$$

Where Zr is the reference height (m), Z is the height for which wind speed is to be determined (m), Zo is the surface roughness (0.1-0.25 for crop land), V(z) is the wind speed at height of z m (m/s), and $V(Zr)$ is the wind speed at the reference height (m/s). Based on the location of the site, the value of Zo has been taken as 0.2.

The extrapolated annual wind speed data obtained from the NMA at 10 m height for Hawassa IP, Kombolcha IP, and Adama IP were 1.65, 1.72, and 2.85 m/s, respectively.

The estimated annual average wind speed data taken from the NASA data base for the three sites were 2.48, 2.5, and 3.57 m/s at 10 m height [55]. These wind speed values are relatively high compared with the NMA data. In general, measurements at 2 m height are error prone due to different kinds of shading and vegetation. Therefore, the data obtained from NASA were considered for this study. The probable monthly average wind speed for the locations at 10m and 50m are given in Fig.7 and Fig.8, respectively.

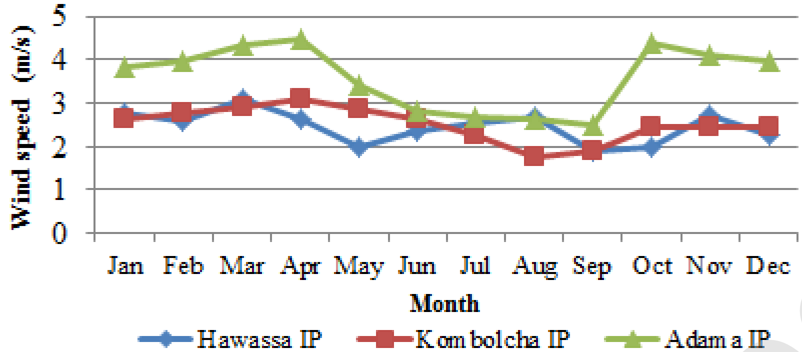

Fig.7. Monthly average wind speed at 10 m height.

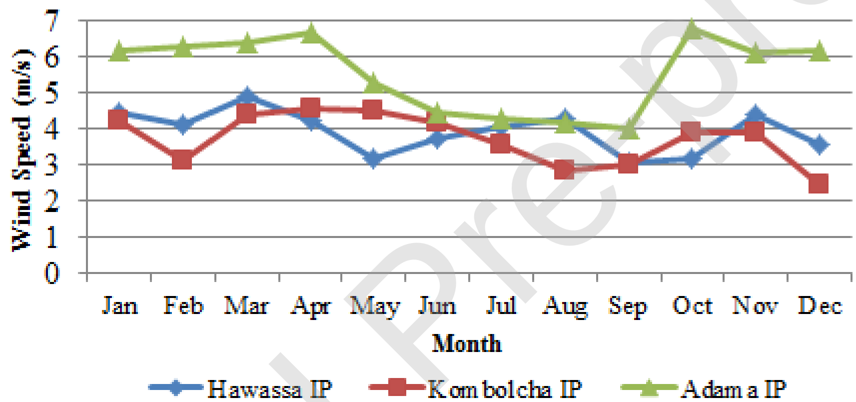

Fig.8. Monthly average wind speed at 50m height.

3.2. Load profile of the location

The total load profiles for the sites were obtained from the respective regions of Ethiopian Electric Utility (EEU) for the year 2018. According to the collected load data, the estimated average daily electricity consumption of the parks was 72 MWh, 43 MWh and 38 MWh. Out of this load an average of 329 kWh/day, 321 kWh/day, and 208 kWh/day consumptions were considered as a critical load, as shown in Fig.9. The unreliable grid and standby diesel generator supplied these critical loads. The remaining loads were supplied only by an unreliable grid. The proposed grid-tied PV/Wind power systems were also modeled by considering the critical load of the sites only.

Based on their product size, the load profiles of the three IPs are different. Peak load demand occurred from 8:00 to 17:00 h in the day. This was mainly because of all the industrial park had started their manufacturing process. The monthly average critical load profiles are shown in Fig.10, Fig.11, and Fig.12 below.

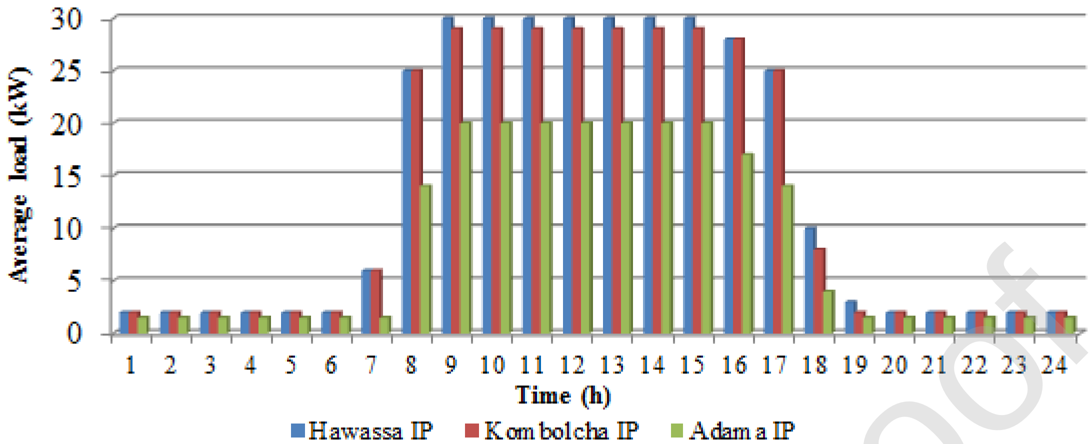

Fig.9. The average daily critical load profile of the parks (year 2018).

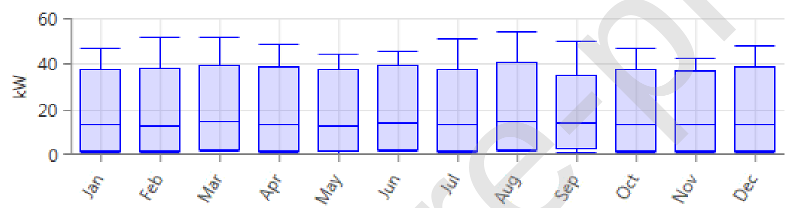

Fig.10. Monthly average critical load profile of Hawassa IP (year 2018).

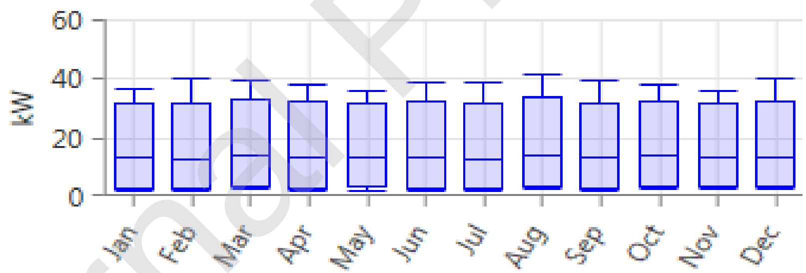

Fig.11. Monthly average critical load profile of Kombolcha IP (year 2018).

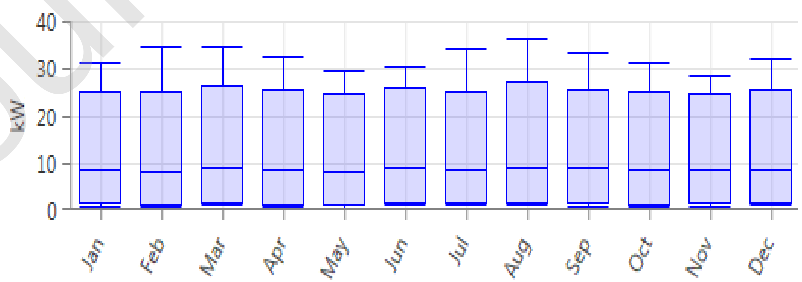

Fig. 12. Monthly average critical load profile of Adama IP (Year 2018).

3.3. Grid outage

In order to design a reliable system with the optimum size of distributed generation, knowing the exact value of interruption data is very important. During this investigation, the line interruption duration and interruption frequency of the sites for the year of 2018 have been collected from EEU of each region. The collected data are shown in Table 2.

Table 2: yearly average interruption of the industry parks.

Name of feeder	Year	Average interruption frequency (Int/year)	Average interruption duration (hr/year)
Hawassa IP	2018	61	92
Kombolcha IP	2018	94	236
Adama IP	2018	89	167

3.3.1. Electricity tariff in the country

The current average electricity tariff is around 0.04 $/kWh, which is one of the lowest cost of energy in Africa [58]. So far, the tariff in the country is subsidized by the government.

3.4. Description of the grid-connected PV/Wind power systems

The proposed scheme set out in Fig.13 foresees the addition of solar PV, wind turbine, battery bank, and convertors to support the diesel generators during outage and to increase the grid sales during normal operation. The representation of Fig.13, after modelled by HOMER Pro for the study regions, is shown in Fig.14.

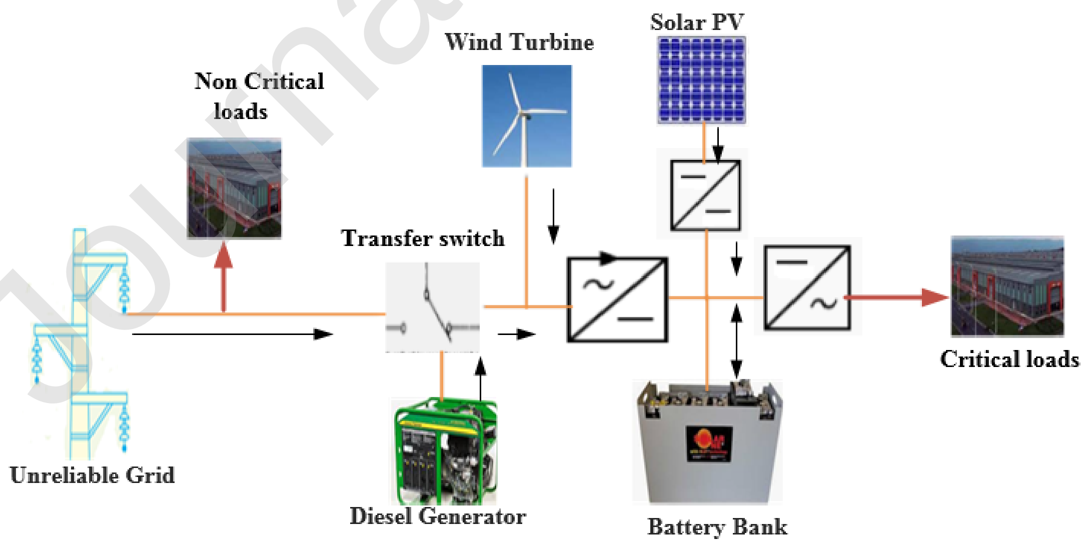

Fig.13. General scheme of the proposed grid-tied PV/Wind systems.

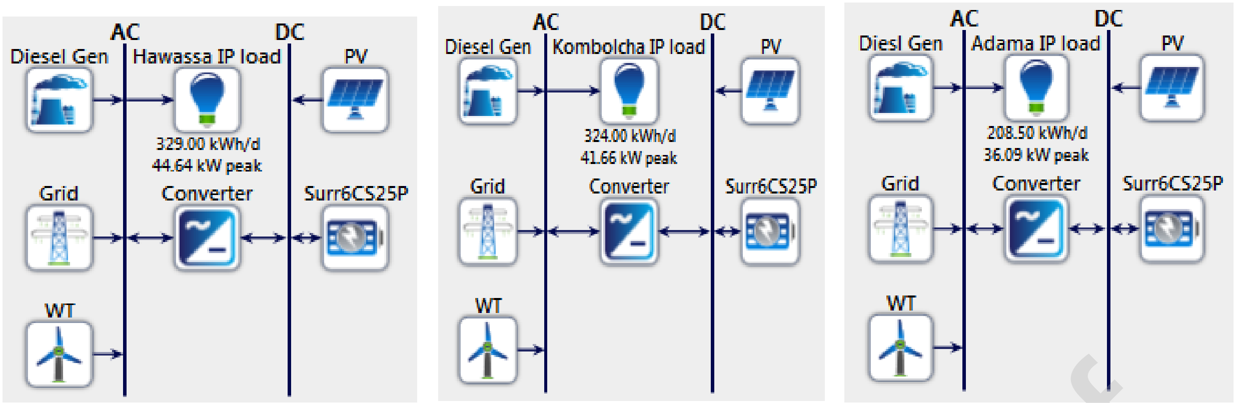

(a) Hawassa IP (b) Kombolcha IP (c) Adama IP

Fig.14. Schematic diagram of grid-connected power system in HOMER Pro for the study regions.

3.4.1. Grid modeling

HOMER Pro allows to model unreliable grid by considering scheduled and unscheduled outages. In this study, an unreliable grid model with unscheduled grid outage was considered. In order to model an unreliable grid with unscheduled outage, mean failure frequency, mean repair time, and variability in repair time are given as an input. Based on the given input and by selecting a pseudo-random time step from a full year simulation period, random outages were generated by the software. Unscheduled grid outages imported from the software simulations are shown in Fig.15, Fig.16, and Fig.17. From the figures, the black spot indicates the random outage throughout the year and the regular grid operation appears in a green. During these outages, the distributed generators are forced to be on.

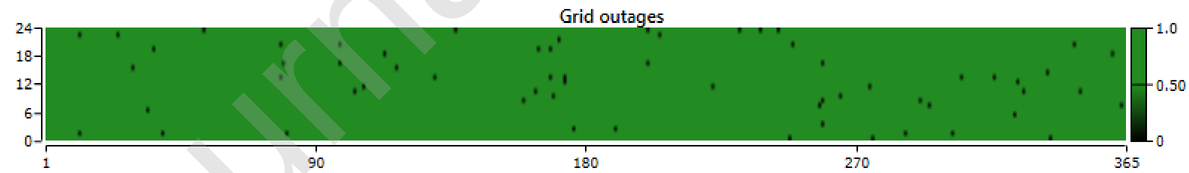

Fig.15. Random grid outages in HOMER for Hawassa IP.

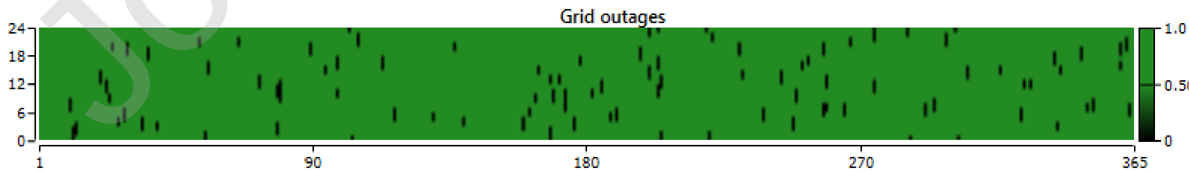

Fig.16. Random grid outages in HOMER for Kombolcha IP.

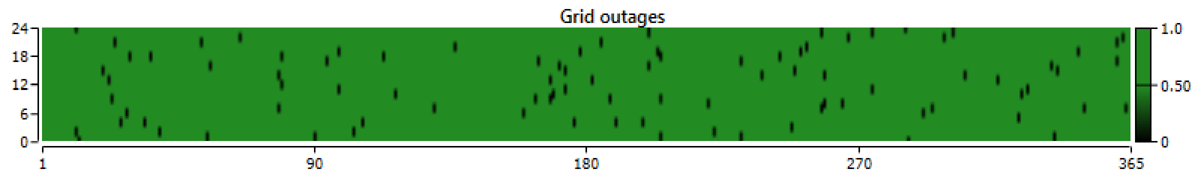

Fig .17. Random grid outages in HOMER for Adama IP.

3.4.2. Solar photovoltaics

The PV panel is modeled as a component that generates DC power in direct proportion to the solar radiation. The output power obtained from the PV module is given by the following equation [59–61]:

$$P_{pv} = Y_{pv} f_{pv} \left(\frac{G_T}{G_{T.STC}}\right)\left[1 + \alpha_p (T_C - T_{c.STC})\right] \quad (7)$$

Where: Y_{pv} is the peak power output [kW], f_{pv} is the PV derating factor, G_T is the solar radiation incident on the PV array in the current time step [kW/m^2], $G_{T.STC}$ is the incident radiation at standard test conditions [1 kW/m^2], α_p is the temperature coefficient of power [%/ °C], T_C is the PV cell temperature in the current time step [°C], and $T_{c.STC}$ is the PV cell temperature under standard test conditions [25 °C].

If the effect of temperature on the PV array is not considered, the temperature coefficient of power is zero; thus, the above equation is simplified into Eq. (8):

$$P_{pv} = Y_{pv} f_{pv} \left(\frac{\bar{G}_T}{\bar{G}_{T.STC}}\right) \quad (8)$$

In this investigation, the effect of temperature is taken into account. The specifications for the selected PV panel in this study are given in Table 3. The capital cost of solar PV is given based on the current local price in the country.

Table 3: Solar PV module technical and economic data.

Parameter	Specification
Panel type	Flat plate
Operating temperature	47 °C
Temperature coefficient of power	-0.40°C
Nominal operating cell temperature	17.02%
Derating factor	0.85
Capital cost	800 $/kW
Operation and maintenance cost	8 $/kW/yr.
Lifetime	25 years

3.4.3. Wind turbine

A wind turbine operates by converting the kinetic energy in the wind first into mechanical power, and the generator converts the mechanical power into electric power. The actual power available in the wind turbine is given by Eq. (9) [62,63].

$$P = \frac{1}{2}\ \rho\, A_T V^3\ Cp \qquad (9)$$

Where P is the output power (W), ρ is the density of air (kg/m^3), A_T is the swept area (m^2), V is the wind speed (m/s^2), and Cp is the power coefficient. To check the viability of the site for wind power production, 10 kW wind turbine is selected. The power-speed characteristic curves and the technical specifications of the selected turbine are given in Fig.18 and Table 4, respectively.

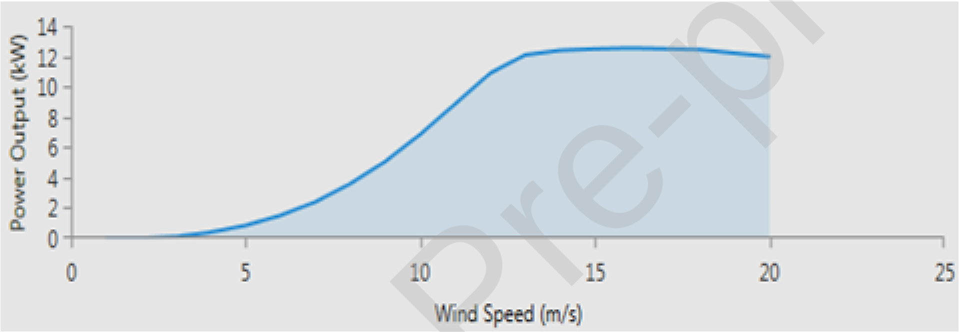

Fig.18. The power-speed characteristic curve of Bergey 10 kW wind turbine.

Table 4: Technical and cost data of the selected wind turbine.

Parameter	Specification
Model	Bergey XL10
Rated power	10 kW
Cut-in wind speed	3 m/s
Cut-off wind speed	20 m/s
Hub height	30 m
Capital cost /unit	35,000 $
Replacement cost /unit	30,000 $
Operation and maintenance cost/unit	1,000 $/year
Lifetime	20 years

3.4.4. Battery

Battery stores direct current (DC) electrical energy in electrochemical form for supporting distributed generators. In addition to supporting the renewable resource, the battery Storage system can improve the grid power quality [64]. Surrette 6CS25P battery model that are appropriate for renewable systems were chosen for this study. The minimum a state of charge point for the batteries has been set at (40%). When this point is reached, the battery does not discharge to avoid the damage with excessive discharge. The discharging and charging equation of the battery is given by Eq. (9) and (10) [60,65].

For battery discharging

$$E_{bt}(t) = E_b(t-1) * (1-\sigma) - [E_{bh}(t) / n_{bi} - E_{bl}(t)] \quad (9)$$

For battery charging

$$E(t) = E_b(t-1) * (1-\sigma) + [E_{bh}(t) - E_{bl}(t) / n_{bi}) * n_{bb}] \quad (10)$$

Where Eb is the battery energy in time interval, E_{bh} is the total energy generated by PV array, E_{bl} is the load demand in time interval, n_{bi} is the inverter efficiency, n_{bb} is the battery charging efficiency, and σ is the self-discharging factor. The technical specifications of the selected battery are listed in Table 5.

3.4.5. Power convertor

A converter is used to convert electric power from DC to AC in a process called inversion and from AC to DC in a process called rectification. Both conversion processes are important. The efficiency of inverter and rectifier is taken as 95% [66,67] . The specifications of the selected converter for this study are given in Table 6.

Table 5: Technical and economic data of the selected battery.

Parameter	Specification
Model	Surrette 6CS25P
Nominal voltage	6V
Maximum capacity	1156 Ah
Minimum state of charge	40%
Roundtrip efficiency	80%
Lifetime throughput	9645Ah
Capital cost	900 $
Replacement cost	700 $
Operation and maintenance cost	9 $/year

Table 6: Cost and technical data of the converter.

Parameter	Specification
Capital cost	650 $
Replacement cost	600 $
Operation and maintenance cost	6 $/year
Efficiency	95%
lifetime	15 years

3.4.6. Diesel generator

A diesel generator is an ancillary component of the existing supply system, and it consumes diesel fuel to produce electricity. The fuel consumption of the generator as a function of its electrical power output is given by the following equation [68,69].

$$F = F_O Y_{gen} + F_1 p_{gen} \qquad (11)$$

Where F is fuel consumption (L/hour), F_0 is generator fuel curve intercept coefficient (L/hr/KW_{rated}), F_1 is the fuel curve slope in L/hr/kW_{output}, $Ygen$ is the rated capacity of the generator in kW, and P_{gen} is the electrical output of the generator in kW. The technical data of the existing diesel generator operating in the industrial parks are presented in Table 7. The capital cost is not considered because the generators have been already installed.

Table 7: Technical and economic data of considered diesel generator in three industry parks.

Parameter	Specification
Generator type	Synchronous
Rated power	50kW, 50kW,48kW
Capital cost	0
Operation and maintenance cost	0.5 $/hour
Diesel price in the country	0.62 $/liter
lifetime	25,000 hours

3.5. System economics

Once the resource and the component data are entered, HOMER Pro ranks all optimization results according to their total net present costs (NPC). The NPC is analyzed with the help of the following equation [27,66,70]:

$$\mathrm{NPC} = \frac{\mathrm{C_T}}{\mathrm{CRF\ (i, N)}} \qquad (12)$$

Where $\mathrm{C_T}$ is the total annualized cost ($/year), i is the annual real interest rate (%), N is the lifetime of the project (year), which taken as 25 years for the study, and CRF is the capital recovery factor. CRF is calculated using the following equation [71,72]:

$$\mathrm{CRF\ (i, N)} = \frac{\mathrm{i(1+i)^N}}{\mathrm{(1+i)^N - 1}} \qquad (13)$$

The annual real interest rate is calculated from the nominal interest rate and inflation rate using the following equation [73,74]:

$$\mathrm{i} = \frac{i_n - \mathrm{f}}{1+\mathrm{f}} \qquad (14)$$

Where i_n is the nominal interest rate (%), and f is the annual inflation rate (%). In this study, a 12.75% nominal interest rate and a 10.84 % annual inflation rate is taken [75]. With these values, using Eq. (14), the real interest rate is found to be **1.72 %.**

The levelized cost of energy (COE) is the per kWh cost of the power plant over an assumed duty cycle and, is calculated as follows [76,77]:

$$COE = \frac{C_T}{E_P + E_d + E_{gs}} \tag{15}$$

Where E_P is the total amount of primary load that the system serves per year (kWh/yr), E_d is the total amounts of deferrable load that the system serves per year (kWh/yr), and E_{gs} is the amount of energy sold to the grid per year (kWh/yr).

4. Simulation result and discussion

Based on the available energy resources and the load demand, HOMER Pro simulates every feasible power supply configuration. In the following subsections, the techno-economic and environmental feasibility analysis of grid/diesel, grid/diesel//PV/battery, grid/PV/battery, and grid/diesel/wind/PV/battery power systems configuration to supply the industrial park load in three different regions of Ethiopia were simulated. Optimization and sensitivity analysis are the two basic simulation results that can be performed by HOMER Pro.

4.1. Optimization results

4.1.1. Grid/diesel generator systems

Grid/diesel generator systems were simulated and analyzed for comparison purposes. In this scenario, diesel generator is fully accountable for supplying the critical loads of the parks during a grid outage. The average monthly electric production from grid/diesel systems for the study regions are shown in Table 8.

Table 8: Monthly average electric production of grid/diesel systems in the three study regions.

Month	Hawassa IP		Kombolcha IP		Adama IP	
	Grid (kW)	Diesel (kW)	Grid (kW)	Diesel (kW)	Grid (kW)	Diesel (kW)
Jan	33.20	3.43	32.41	5.11	24.21	4.35
Feb	33.13	3.31	32.31	4.58	25.03	3.56
Mar	33.45	3.89	32.48	4.79	25.50	3.23
Apr	33.14	3.59	32.53	5.98	25.21	4.21
May	33.00	1.98	32.52	4.43	24.92	3.10
Jun	33.23	4.98	32.80	5.64	25.23	4.34
July	33.12	1.92	32.69	5.43	26.02	4.10
Aug	33.85	2.11	33.11	4.50	25.11	4.15
Sep	33.21	3.82	32.80	5.19	25.01	3.75
Oct	33.20	3.78	32.69	3.85	24.51	2.64
Nov	33.00	4.51	32.59	5.19	24.29	4.43
Dec	33.14	3.97	32.62	5.79	24.21	4.32

Economic and environmental considered output of the grid/diesel systems for the investigated locations are shown in Table 9 and Table 10. Without considering the capital and replacement costs, the NPC and COE of the three regions of grid/diesel systems were $102,290 and 0.042 $/kWh (Hawassa IP), $116,123 and 0.048 $/kWh (Kombolcha IP) and $73,511 and 0.047 $/kWh (Adama IP). These systems produce a total of 1,174 kg/yr, 4,459 kg/yr, and 2,533 kg/yr gas emission in Hawassa, Kombolcha, and Adama, respectively.

Table 9: Economic characteristics of optimized grid/diesel systems.

Location	System	Grid (kW)	Diesel (kW)	NPC ($)	COE ($/kWh)	RF
Hawassa IP	grid/diesel	80	50	102,290	0.042	0
Kombolcha IP	grid/diesel	80	50	116,123	0.048	0
Adama IP	grid/diesel	80	48	73,511	0.047	0

Table 10: Annual emissions (kg/yr) from diesel generator during grid/diesel systems operation.

Location	CO_2	CO	NO_2	SO_2	PM	Unburned Hydrocarbon	Total Emissions (kg/yr)
Hawassa IP	1,155	8.13	7.05	2.95	0.05	0.38	1,174
Kombolcha IP	4,394	27.21	25.31	10.81	0.16	1.21	4,459
Adama IP	2,495	16.1	14.91	6.11	0.09	0.69	2,533

The annual energy production from grid/diesel systems and annual consumption for the three regions are shown in Table 11.

Table 11: Annual electric production and consumption of the three regions.

Locations	Grid Purchase (kWh/year)	Diesel generation (kWh/year)	Load (kWh/year)
Hawassa IP	118,998	1,295	119,885
Kombolcha IP	114,365	4,679	118,102
Adama IP	74,168	2,674	76,102

4.1.2. Grid/diesel/PV/battery systems.

In this system architecture, PV/battery systems help the diesel generator during a grid outage. The monthly average electric productions from grid/diesel/PV/battery systems for the three regions are shown in Table 12. The minimum and maximum monthly power production from the grid and diesel are also shown in this table. In general when we observe the three locations, the PV systems were capable enough to produce a power throughout the year in all three climate zones.

Table 12: Monthly average electric production of grid/diesel/PV/battery systems.

Month	Hawassa IP			Kombolcha IP			Adama IP		
	Grid (kW)	Diesel (kW)	PV (kW)	Grid (kW)	Diesel (kW)	PV (kW)	Grid (kW)	Diesel (kW)	PV (kW)
Jan	29.65	1.45	7.12	28.95	2.98	7.75	22.30	2.50	4.58
Feb	28.05	0.68	8.01	28.48	3.14	6.55	21.98	1.00	4.88
Mar	30.00	1.54	7.14	29.45	2.99	7.65	22.20	1.23	4.60
Apr	30.00	2.13	6.95	29.10	2.89	8.00	21.99	2.40	4.57
May	29.99	1.56	7.01	29.00	3.49	6.78	21.98	2.50	4.53
Jun	30.12	2.13	6.93	29.01	3.41	7.75	22.20	2.71	4.31
Jul	31.11	3.32	6.01	29.12	3.51	6.60	22.35	2.87	4.10
Aug	31.01	3.15	6.10	31.23	3.99	6.20	23.50	3.82	3.70
Sep	29.93	2.98	6.23	29.98	3.89	6.58	22.43	3.12	4.22
Oct	30.00	1.59	7.00	29.42	3.75	6.55	22.23	2.71	4.58
Nov	29.87	1.56	7.11	28.99	3.84	6.53	21.67	2.79	4.57
Dec	29.78	1.41	7.17	28.89	2.65	7.51	22.24	2.74	4.30

The economic and annual emission characteristics of the optimized grid/diesel/PV/battery systems for the study regions are shown in Table 13 and Table 14. Because of the highest grid outage and highest consumption from diesel generator in Kombolcha IP, the NPC ($116,998) of the systems was also the highest among the three regions. The lowest NPC ($74,044) was observed in Adama IP. Lowest emissions were observed in Hawassa IP due to the lowest grid outage consideration. The highest emissions were found in Kombolcha IP.

Table 13: Economic characteristics of optimized grid/diesel/PV/battery systems.

Location	System	Grid (kW)	Diesel (kW)	PV (kW)	Battery	Converter (kW)	NPC ($)	COE ($/kWh)	RF
Hawassa IP	grid/diesel/PV/ battery	80	50	10	4	6	107,855	0.044	13.3
Kombolcha IP	grid/diesel/PV/ battery	80	50	10	6	6	116,998	0.049	13.4
Adama IP	grid/diesel/PV/ battery	80	48	6	3	4	74,044	0.048	12.9

Table14: Annual emissions (kg/yr) from diesel generator for grid /diesel/PV/battery systems.

Location	CO_2	CO	NO_2	SO_2	PM	Unburned Hydrocarbon	Total Emissions (kg/yr)
Hawassa IP	640	4.53	4.12	1.89	0.038	0.247	651
Kombolcha IP	2,444	15.6	14.3	5.98	0.092	0.672	2,475
Adama IP	1,449	9.36	8.68	3.55	0.055	0.399	1,471

The summery of annual energy production from grid/diesel/PV/battery systems and annual consumption for the three regions are shown in Table 15.

Table 15: Annual electric production and consumption of the three regions.

Locations	Grid Purchase (kWh/year)	Diesel generation (kWh/year)	PV Generation (kWh/year)	Load (kWh/year)	Grid sales (kWh/year)	Total consumption (kWh/year)
Hawassa IP	102,890	698	18,041	119,885	35.78	119,921
Kombolcha IP	99,112	2,634	17,405	118,102	12.5	118,115
Adama IP	64,768	1,545	10,864	76,102	26	76,128

4.1.3. Grid/PV/battery systems.

Among the common possible combination in three regions, the NPC and COE of grid/PV/battery systems were the highest. However, there is no emission in this configuration. The economic characteristics of the systems are shown in Table 16.

Table 16: Economic characteristics of optimized grid/PV/battery systems.

Location	System	Grid (kW)	PV (kW)	Battery	Converter (kW)	NPC ($)	COE ($/kWh)	RF
Hawassa IP	grid/PV/battery	80	30	20	25	136,151	0.056	41.6
Kombolcha IP	grid/PV/battery	80	35	25	35	151,432	0.060	48.2
Adama IP	grid//PV/battery	80	25	20	25	104,120	0.063	49.6

4.1.4. Grid/diesel/wind/PV/battery systems.

From the three regions, wind power was technically and environmentally feasible only in Adama IP. However, the COE for wind integrated power systems was considered as the highest among all possible configurations for this region. The economic and environmental oriented outputs of the systems are shown in Table 17 and Table 18.

Table 17: Economic output of optimized grid/diesel/PV/wind/battery systems.

Location	Systems	Grid (kW)	Diesel (kW)	PV (kW)	Wind (kW)	Battery	Converter (kW)	COE ($/kWh)	RF
Adama IP	grid/diesel/wind/ PV/battery	80	48	6	10	3	4	0.081	22.1

Table18: Annual emissions (kg/yr) from diesel generator for grid/diesel/PV/wind/battery systems.

Location	CO_2	CO	NO_2	SO_2	PM	Unburned Hydrocarbon	Total Emissions (kg/yr)
Adama IP	1,270	8.50	7.94	3.20	0.046	0.320	1,290

4.1.5. Economic and environmental comparative analysis of the proposed four systems

In order to select the best supply option for the locations from the proposed scenario, the economic and environmental-related parameter comparison is essential. The economic and emission parameter that serves as a feasibility determinant factors for each regions are shown in Table 19. For all three climate regions, the grid/diesel systems were the lowest cost systems; however, the total annual emissions of systems were the highest. Emissions from grid/diesel/PV/battery systems were lower than grid/diesel systems for all regions. Grid /PV/battery systems are emission free systems, but the COE of the grid /PV/battery systems were higher than the COE of grid/diesel/PV/battery systems. The COE of grid /diesel/wind/battery systems were the highest among the considered supply option in the region.

Table 19: A comparison between the four scenarios for the three regions.

Systems	Hawassa IP			Kombolcha IP			Adama IP		
	NPC	COE ($/kWh)	Annual emission (kg /yr)	NPC ($)	COE ($/kWh)	Annual emission (kg /yr)	NPC ($)	COE ($/kWh)	Annual emission (kg /yr)
grid/diesel	102,290	0.042	1,174	116,123	0.048	4,459	73,511	0.047	2,533
grid/diesel/ PV/battery	107,855	0.044	651	116,998	0.049	2,475	74,044	0.048	1,471
grid/PV/ battery	136,151	0.056	0	151,432	0.060	0	104,120	0.063	0
grid/diesel/ wind/PV/ battery	-	-	-	-	-	-	129, 125	0.081	1,290

4.2. Sensitivity analysis results

Sensitivity analysis indicates the effect of changing multiple values for a particular input variable on the optimal system design. Such variables can be solar radiation, PV capital cost, grid tariff, load demand, fuel prices, grid outage, and any other related parameters that might affect the economic output of the optimal system. In this investigation, the effects of electric load change, solar radiation, grid tariff, and grid outage on the NPC and COE for the optimal system design of grid/diesel/PV/battery systems were explored.

4.2.1. Effect of load change

As it is stated in section 3.2 previously, the daily average critical load demands of the sites are considered as 329 kWh/day (Hawassa IP), 321 kWh/day (kombolcha IP), and 208 kWh/day (Adama IP). However, by considering the dynamic nature of the loads, the energy demands of the three regions are varied from 300 kWh /day to 380 kWh/day for Hawassa IP and kombolcha IP and 200 kWh/day to 280 kWh/day for Adama IP. The performance of total NPC and COE has been measured accordingly. As shown in Fig.19, the NPC of the systems for all three sites increased with increasing load demand, whereas the COE decreased with increasing load demand.

4.2.2. Effect of solar radiation variations

Figure 20 shows the results of sensitivity analyses of the optimized grid/diesel/PV/battery systems to variations in solar radiation. The load (329 kWh/day, 321 kWh/day and 208 kWh/day for the Hawassa IP, Kombolcha IP, and Adama IP) and grid power price (0.04 $/kWh) were all fixed simultaneously. The NPC values of the three locations decreased as global solar radiation values increased, but the RF values of these three locations increased as the solar radiation increased. This suggests that solar PV penetration in the grid is very important for reducing energy-related environmental concerns.

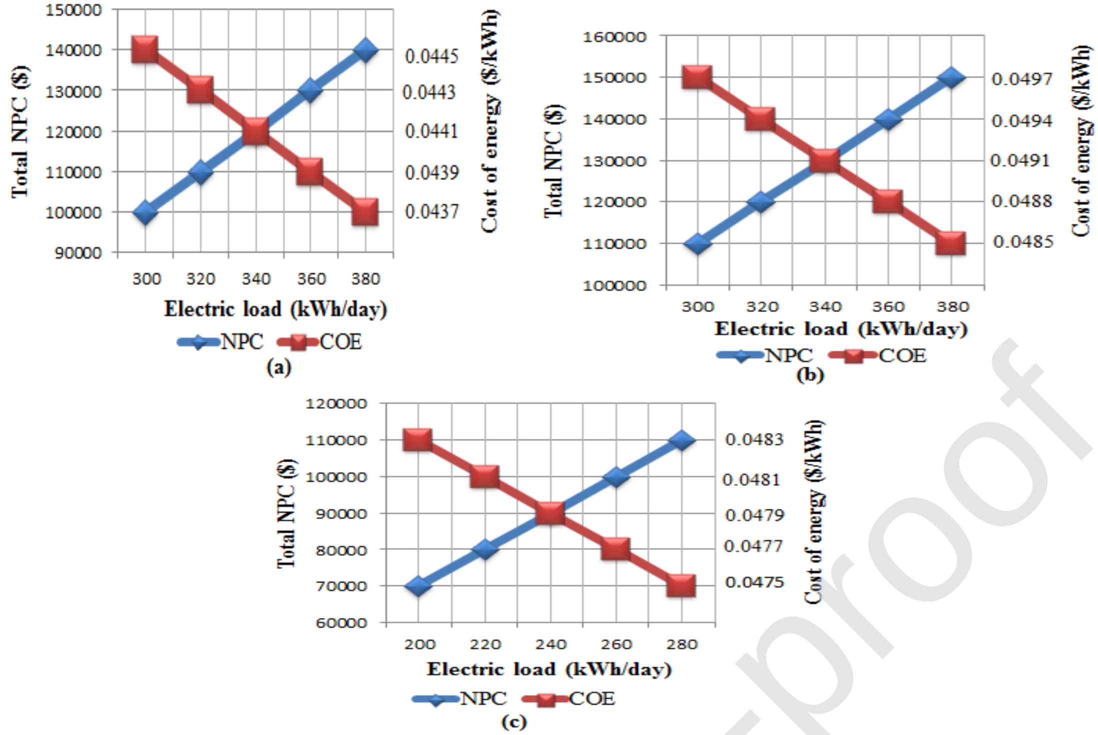

Fig.19. Effect of electric load change on the NPC and COE for the study regions ((a) Hawassa IP, (b) Kombolcha IP, and (c) Adama IP).

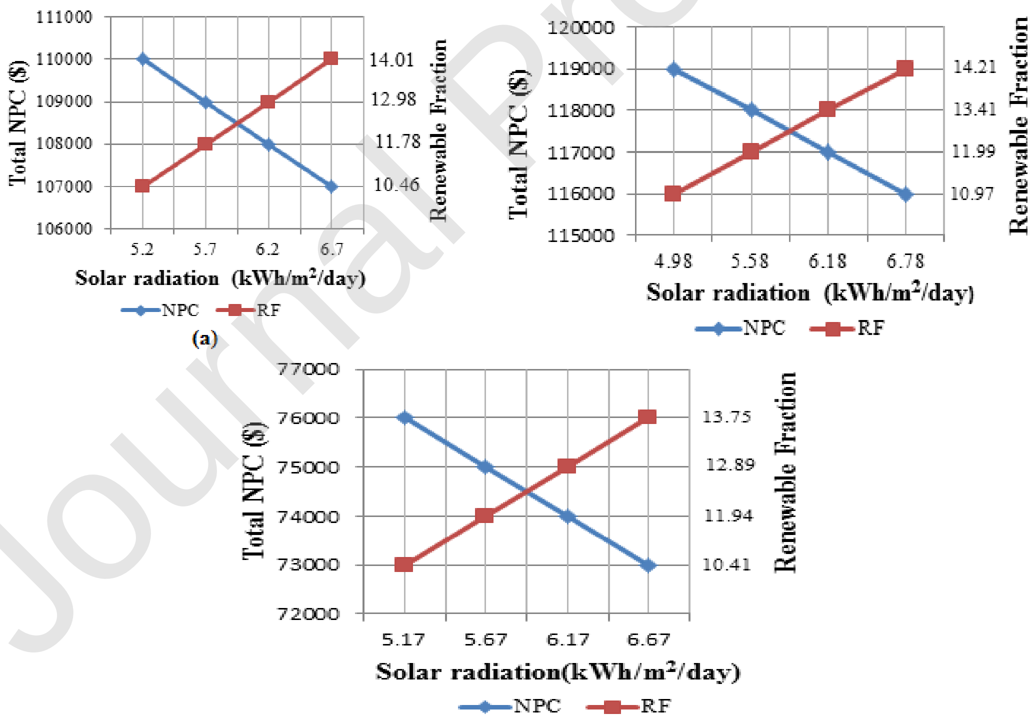

Fig.20. Effect of solar radiation variation on the NPC and RF for the study regions ((a) Hawassa IP, (b) Kombolcha IP, and (c) Adama IP).

4.2.3. Effect of grid power price variations

The grid tariff is varied from 0.04 $/kWh to 0.07 $/kWh for all regions. The NPC and the COE of all locations increased with increasing power prices. For all regions, the rate of grid power price at a country level is the same. Therefore, it is enough to see one region as a sample.Fig.21 below shows the effect of grid power price variation on the NPC and COE for Hawassa IP.

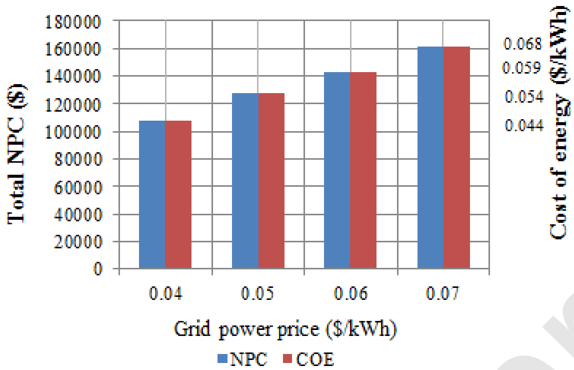

Fig.21. Effect of grid power price on the NPC and COE for the study region.

4.2.4. Effect of grid outage variations

By keeping the total load and the grid power price of each region constant, the line interruption duration of the three regions was varied from 80-110 hr/year for Hawassa IP, 230-260 hr/year for Kombolcha and 160-190 hr/year for Adama IP, respectively. As shown in Fig.22, the NPC and the COE of all sites increased with increasing line interruption duration. In the analysis, the interruption frequency was varied proportionally with the interruption duration, and the unscheduled outage was considered.

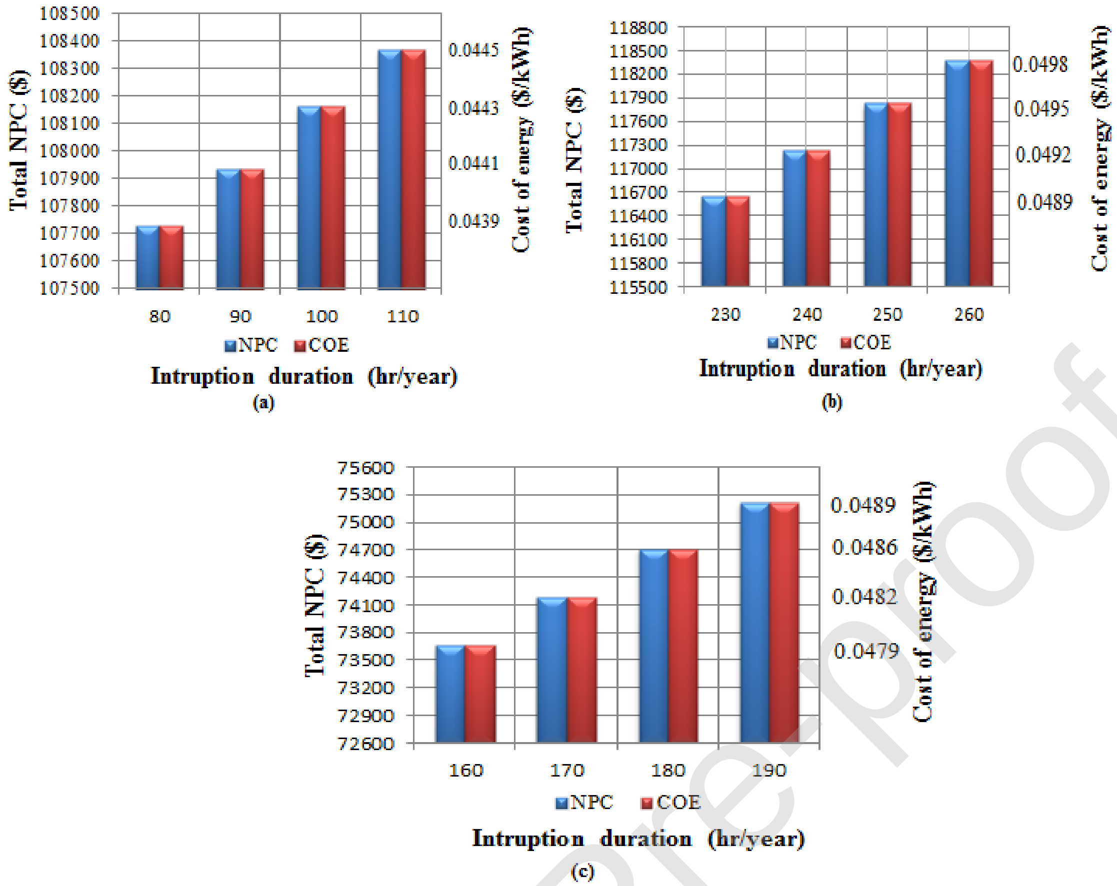

Fig.22. Effect of grid outage variation on the NPC and COE for the study regions ((a) Hawassa IP, (b) Kombolcha IP, and (c) Adama IP).

5. Conclusion

In this paper, the techno-economic feasibility analysis of grid-connected PV/wind power systems considering unreliable grid/diesel systems for the industrial park (IP) load in three different regions of Ethiopia was analyzed. NPC, COE, and emissions were considered as basic parameters to indicate the feasibility of the designed systems.

Based on the objective of the study and by considering the feasibility determinant constraints, the main conclusions of the investigation are presented as follows:

- Solar energy was potentially feasible for all three regions. The analyzed annual average solar radiation for Hawassa IP, Kombolcha IP, and Adama IP were 6.18 kWh/m^2/day, 5.96 kWh/m^2/day, and 6.20 kWh/m^2/day respectively. The annual average temperature for the locations were 27.9 ^{0}C (Hawassa IP) 27 ^{0}C (Kombolcha IP), and 28.14 ^{0}C (Adama IP) ,respectively.

- Except for Adama IP, Hawassa IP and Kombolcha IP locations were not feasible for wind power production. The average annual maximum and minimum wind speed at 50 m for the sites were 4.9 m/s, 3.1 m/s (Hawassa IP), 4.6 m/s, 2.84 m/s (Kombolcha IP) and 6.7 m/s, 3.8 m/s (Adama IP) respectively.
- The grid/diesel systems were the lowest cost systems among the other considered configuration for all three regions, but the emissions for grid/diesel systems were relatively the highest.
- In grid/PV/battery systems there are no emissions; however, the COE of the grid /PV/battery systems was higher than the COE of grid/diesel/PV/battery systems.
- Grid/diesel/wind/PV/battery systems were technically feasible in Adama IP, but the COE of the systems was higher than the remaining possible other configurations of the region.
- Based on technical, economic, and environmental consideration, the grid/diesel/PV/battery systems were the best supply option for all three regions among the considered systems.
- From sensitivity analysis, it is observed that the optimal grid/diesel/PV/battery systems operate reasonably well with the variation of electric load, solar radiation, grid power price, and grid outage variation.
  - ✓ The NPC of the optimal systems for all three regions increased as the electric load increased, and the COE decreased as the electric load increased.
  - ✓ The NPC and the emission of the optimal systems in all three places decreased as the solar radiation increased
  - ✓ The NPC and the COE of the optimal systems in all three sites increased as grid tariff increased.
  - ✓ The NPC and the COE of the optimal systems in all three regions increased as the line interruption duration increased.
- In general, based on the results from this investigation, the implementation of grid-integrated solar PV systems in the south, north-central and central part of Ethiopia could be environmentally and economically viable. Thus, the finding of this research study will provide a convincing pathway to the concerned stakeholders and policy makers to extend these systems into the aforementioned regions for application to other firms also.

Declaration of interests

☒ The authors declare that they have no known competing financial interests or personal relationships that could have appeared to influence the work reported in this paper. In short, the authors declare they have no conflict of interest.

Acknowledgements

The authors would like to thank Ethiopian National Meteorology Agency and Ethiopian Electric Utility for their cooperation to provide the meteorological, load, and grid data. The authors are also thankful to the National Renewable Energy Laboratories (NREL) for providing the HOMER Pro software free. Last but not least, our exceptional thanks go to Ethiopian Ministry of Science and Higher Education and the German Development Bank (KfW) through ExiST project for funding this research.

Reference

[1] Federal Democratic Republic of Ethiopia , Ministry of water and energy. Scaling - up Renewable Energy Program and Ethiopia Investment Plan. Addis Ababa: 2012.

[2] Ministry Of Water Irrigation and Electricity.The Ethiopian Power Sector: a Renewable Future:Berlin Energy Transition Dialogue. Berlin : 2017.

[3] CIA The world fact book; 2017. <https://www.cia.gov/library/publications/the-world factbook/geos/et.html> [Retrieved on 22-10- 2018].

[4] International Hydropower Association. Hydropower status report. 2018;1–83.

[5] World Bank Enterprise survey; 2015. < http://www.eneterprise .org/data/exploretopics /infrastructure> [Retrieved on 21-10- 2018].

[6] Rodríguez-Gallegos CD, Gandhi O, Bieri M, et al. A diesel replacement strategy for off-grid systems based on progressive introduction of PV and batteries: An Indonesian case study. Appl. Energy. 2018;229:1218–1232.

[7] Carlsson F, Demeke E, Martinsson P. Cost of Power Outages for Manufacturing Firms in Ethiopia : A Stated Preference Study. university of Gothenburg Working Paper in Economics No. 731; May 2018.

[8] Khalife E, Tabatabaei M, Demirbas A, et al. Impacts of additives on performance and emission characteristics of diesel engines during steady state operation. Prog. Energy

Combust. Sci. 2017;59:32–78.

[9] Mohankumar S, Senthilkumar P. Particulate matter formation and its control methodologies for diesel engine: A comprehensive review. Renew. Sustain. Energy Rev. 2017;80:1227–1238.

[10] Wei L, Geng P. A review on natural gas / diesel dual fuel combustion , emissions and performance. Fuel Process. Technol. 2016;142:264–278.

[11] Ramli MAM, Bouchekara HREH, Alghamdi AS. Optimal sizing of PV/wind/diesel hybrid microgrid system using multi-objective self-adaptive differential evolution algorithm. Renew. Energy. 2018;121:400–411.

[12] Hossain M, Mekhilef S, Olatomiwa L. Performance evaluation of a stand-alone PV-wind-diesel-battery hybrid system feasible for a large resort center in South China Sea ,. Sustain. Cities Soc. 2017;28:358–366.

[13] World Bank, Ethiopia electrification program report; 2018. <<http://documents. world bank.org/ curated/en/ 686501520132423023 /pdf/ETHIOPIA -PAD -02092018.pdf>> [Retrieved on 29-8- 2018].

[14] Federal Dmocratic Republic of Ethiopia, Report on Ethiopia's climate resilient green Economy ; 2013. <<http://www.adaptation-undp .org /sites/default /files /downloads /ethiopia_climate _resilient_green_economy_strategy.pdf>> [Retrieved on 21-9-2018].

[15] Numbi BP, Malinga SJ. Optimal energy cost and economic analysis of a residential grid-interactive solar PV system- case of eThekwini municipality in South Africa. Appl. Energy. 2017;186:28–45.

[16] International renewable energy agency (IRENA), Report on renewable energy policies in a time of transition; 2018. <<https://www.irena.org/-/media/Files/IRENA/Agency/Publi cation /2018 /Apr/IRENA_IEA_REN21_Policies_2018.pdf>> [Retrieved on 02-9- 2018].

[17] Islam MS. A techno-economic feasibility analysis of hybrid renewable energy supply options for a grid-connected large office building in southeastern part of France. Sustain. Cities Soc. 2018;38:492–508.

[18] Rehman S, Ahmed MA, Mohamed MH, et al. Feasibility study of the grid connected 10 MW installed capacity PV power plants in Saudi Arabia. Renew. Sustain. Energy Rev. 2017;80:319–329.

[19] Gonzalez A, Riba JR, Esteban B, et al. Environmental and cost optimal design of a biomass–Wind–PV electricity generation system. Renew. Energy. 2018;126:420–430.

[20] Li C, Zhou D, Zheng Y. Techno-economic comparative study of grid-connected PV power systems in five climate zones, China. Energy. 2018;165:1352–1369.

[21] Kazem HA, Albadi MH, Al-waeli AHA, et al. Techno-economic feasibility analysis of 1 MW photovoltaic grid connected system in Oman. Case Stud. Therm. Eng. 2017;10:131–141.

[22] Bastholm C, Fiedler F. Techno-economic study of the impact of blackouts on the viability of connecting an o ff -grid PV-diesel hybrid system in Tanzania to the national power grid. Energy Convers. Manag. 2018;171:647–658.

[23] Al Garni HZ, Awasthi A, Ramli MAM. Optimal design and analysis of grid-connected photovoltaic under different tracking systems using HOMER. Energy Convers. Manag. 2018;155:42–57.

[24] Rehman SU, Rehman S, Shoaib M, et al. Feasibility Study of a Grid-Tied Photovoltaic System for Household in Pakistan: Considering an Unreliable Electric Grid. Environ. Prog. Sustain. Energy. 2018;

[25] Jahangiri M, Haghani A, Alidadi A, et al. Feasibility study on the provision of electricity and hydrogen for domestic purposes in the south of Iran using grid-connected renewable energy plants. Energy Strateg. Rev. 2019;23:23–32.

[26] Mukisa N, Zamora R, Lie TT. Feasibility assessment of grid-tied rooftop solar photovoltaic systems for industrial sector application in Uganda. Sustain. Energy Technol. Assessments. 2019;32:83–91.

[27] Haratian M, Tabibi P, Sadeghi M, et al. A renewable energy solution for stand-alone power generation: A case study of KhshU Site-Iran. Renew. Energy. 2018;125:926–935.

[28] Zhang W, Maleki A, Rosen MA, et al. Optimization with a simulated annealing algorithm of a hybrid system for renewable energy including battery and hydrogen storage. Energy. 2018;163:191–207.

[29] Sanajaoba Singh S, Fernandez E. Modeling, size optimization and sensitivity analysis of a remote hybrid renewable energy system. Energy. 2018;143:719–731.

[30] Fulzele J, Diagavane M. Des ign and Optimization of Hybrid PV-Wind Renew wable En nergy system. Mater. TodayProceedings. 2018;5:810–818.

[31] Fodhil F, Hamidat A, Nadjemi O. Potential , optimization and sensitivity analysis of photovoltaic-diesel-battery hybrid energy system for rural electri fi cation in Algeria. Energy. 2019;169:613–624.

[32] Das BK, Zaman F. Performance analysis of a PV / Diesel hybrid system for a remote area in Bangladesh : Effects of dispatch strategies , batteries , and generator selection. Energy. 2019;169:263–276.

[33] Halabi LM, Mekhilef S, Olatomiwa L, et al. Performance analysis of hybrid PV / diesel / battery system using HOMER : A case study Sabah , Malaysia. Energy Convers. Manag. 2017;144:322–339.

[34] Razmjoo A, Shirmohammadi R, Davarpanah A, et al. Stand-alone hybrid energy systems for remote area power generation. Energy Reports. 2019;5:231–241.

[35] Olatomiwa L, Mekhilef S, Huda ASN, et al. Economic evaluation of hybrid energy systems for rural electri fi cation in six geo-political zones of Nigeria. Renew. Energy.

2015;83:435–446.

[36] Mandal S, Das BK, Hoque N. Optimum Sizing of a Stand-alone Hybrid Energy System for Rural Electrification in Bangladesh. J. Clean. Prod. 2018;200:12–27.

[37] Olatomiwa L, Blanchard R, Mekhilef S, et al. Hybrid renewable energy supply for rural healthcare facilities: An approach to quality healthcare delivery. Sustain. Energy Technol. Assessments. 2018;30:121–138.

[38] Tawfik TM, Badr MA, El-Kady EY, et al. Optimization and energy management of hybrid standalone energy system: a case study. Renew. Energy Focus. 2018;25:48–56.

[39] Olatomiwa L, Mekhilef S, Huda ASN, et al. Techno-economic analysis of hybrid PV – diesel – battery and PV – wind – diesel – battery power systems for mobile BTS : the way forward for rural development. Energy Sci. Eng. 2015;271–285.

[40] Jamshidi M, Askarzadeh A. Techno-economic analysis and size optimization of an o ff - grid hybrid photovoltaic , fuel cell and diesel generator system. Sustain. Cities Soc. 2019;44:310–320.

[41] Shezan SKA, Das N, Mahmudul H. Techno-economic analysis of a smart-grid hybrid renewable energy system for Brisbane of Australia Cost of Energy. Energy Procedia. 2017;110:340–345.

[42] Zhou B, Xu D, Li C, et al. Multiobjective Generation Portfolio of Hybrid Energy Generating Station for Mobile Emergency Power Supplies. IEEE Trans. Smart Grid. 2018;9:5786–5797.

[43] Halabi LM, Mekhilef S. Flexible hybrid renewable energy system design for a typical remote village located in tropical climate. J. Clean. Prod. 2018;177:908–924.

[44] Das BK, Hoque N, Mandal S, et al. A techno-economic feasibility of a stand-alone hybrid power generation for remote area application in Bangladesh. Energy. 2017;134:775–788.

[45] Federal Democratic Republic of Ethiopia, National planning commission, Report on Growth and Transformatin Plan II (GTP II) (2015-2020): Addis Ababa:2016.

[46] United Nation Development Organization,Industrial park development in Ethioipa case study report 2018. <https:// www.unido.org/api/opentext/ documents/ download/ 10694802/unido-file 1069480> [Retrieved on 19-10- 2018].

[47] Embassy of Federal Democratic Republic of Ethiopia in Japan,Tokyo. Industrial Parks Development Corporation of Ethiopia: 2016. <https:// www.jetro .go.jp/ext_images/ world/africa/seminar_reports/pdf/20160325/4.pdf> [Retrieved on 15-12-2018].

[48] Ethiopian investment commission, industrial park in Ethiopia: 2017. <http:/ www. invest ethiopia. gov.et./index.php/puplication.html> [Retrieved on 25-10- 2018].

[49] Fazzini M, Bisci C, Billi P. The Climate of Ethiopia. Springer,r Dordrecht; 2015.

[50] Gonfa L. Climatic classification of Ethiopia. National Mapping Authority, Addis Ababa;

1996.

[51] Ethiopian investment commission, Ethiopian investment report: 2017. <http:/ www. invest ethiopia. gov.et./index.php/puplication.html> [Retrieved on 27-10- 2018].

[52] Mulugeta Y, Drake F. Assessment of solar and wind energy resources in Ethiopia. II. Wind energy. Sol. Energy. 1996;57 (4):323–334.

[53] Bekele G, Palm B. Feasibility study for a standalone solar-wind-based hybrid energy system for application in Ethiopia. Appl. Energy. 2010;87:487–495.

[54] Duffie JA, Beckman WA. Solar engineering of thermal processes. 3rd ed. New York: Wiley; 2006.

[55] NASA Prediction of worldwide energy resource; 2018. <http://power.larc.nasa.gov/> [Retreived on 23-12- 2018].

[56] Manwell JF, McGowan JG, Rogers AL. Wind energy explained: theory, design and application.2nd ed. U.K: Wiley; 2009.

[57] Drake F, Mulugetta Y. Assessment of solar and wind energy in Ethiopia. I. Solar energy. Sol Energy 1996; 57 (3):205–17.

[58] Ethiopian Electric utility current tariffs, < http://www.eeu.gov.et/index.php/current-tariff> [Retrieved on 1-02- 2019].

[59] Ismail MS, Moghavvemi M, Mahlia TMI. Techno-economic analysis of an optimized photovoltaic and diesel generator hybrid power system for remote houses in a tropical climate. Energy Convers. Manag. 2013;69:163–173.

[60] Thomas D, Deblecker O, Ioakimidis CS. Optimal design and techno-economic analysis of an autonomous small isolated microgrid aiming at high RES penetration. Energy. 2016;116:364–379.

[61] Soshinskaya M, Crijns-Graus WHJ, van der Meer J, et al. Application of a microgrid with renewables for a water treatment plant. Appl. Energy. 2014;134:20–34.

[62] Mathew S. Wind Energy: Fundamentals, Resource Analysis and Economics. Berlin Heidelberg : Springer-Verlag ; 2006.

[63] Wagner H, Mathur J. Introduction to Wind Energy Systems: Basics, Technology and Operation. Berlin Heidelberg: Springer-Verlag; 2009.

[64] Bahmani-Firouzi B, Azizipanah-Abarghooee R. Optimal sizing of battery energy storage for micro-grid operation management using a new improved bat algorithm. Int. J. Electr. Power Energy Syst. 2014;56:42–54.

[65] Haidar AMA, John PN, Shawal M. Optimal configuration assessment of renewable energy in Malaysia. Renew. Energy. 2011;36:881–888.

[66] Duman AC, Güler Ö. Techno-economic analysis of o ff -grid PV / wind / fuel cell hybrid

system combinations with a comparison of regularly and seasonally occupied households. Sustain. Cities Soc. 2018;42:107–126.

[67] Gökçek M. Integration of hybrid power (wind-photovoltaic-diesel-battery) and seawater reverse osmosis systems for small-scale desalination applications. Desalination. 2018;435:210–220.

[68] Diab F, Lan H, Zhang L, et al. An environmentally friendly factory in Egypt based on hybrid photovoltaic / wind / diesel / battery system. J. Clean. Prod. 2016;112:3884–3894.

[69] Dufo-lo R. Multi-objective design of PV – wind – diesel – hydrogen – battery systems. Renew. Energy. 2008;33:2559–2572.

[70] Sinha S, Chandel SS. Prospects of solar photovoltaic-micro-wind based hybrid power systems in western Himalayan state of Himachal Pradesh in India. Energy Convers. Manag. 2015;105:1340–1351.

[71] Phurailatpam C, Rajpurohit BS, Wang L. Planning and optimization of autonomous DC microgrids for rural and urban applications in India. Renew. Sustain. Energy Rev. 2018;82:194–204.

[72] Singh G, Baredar P, Singh A, et al. Optimal sizing and location of PV, wind and battery storage for electrification to an island: A case study of Kavaratti, Lakshadweep. J. Energy Storage. 2017;12:78–86.

[73] Dursun B. Determination of the optimum hybrid renewable power generating systems for Kavakli campus of Kirklareli University , Turkey. Renew. Sustain. Energy Rev. 2012;16:6183–6190.

[74] Ramli MAM, Hiendro A, Twaha S. Economic analysis of PV / diesel hybrid system with fl ywheel energy storage. Renew. Energy. 2015;78:398–405.

[75] National Bank of Ethiopia: National Bank of Ethiopia Quarterly Bulletin, Volume 34, No. 1: Addis Ababa: 2018.

[76] Zou H, Du H, Brown MA, et al. Large-scale PV power generation in China: A grid parity and techno-economic analysis. Energy. 2017;134:256–268.

[77] Haghighat Mamaghani A, Avella Escandon SA, Najafi B, et al. Techno-economic feasibility of photovoltaic, wind, diesel and hybrid electrification systems for off-grid rural electrification in Colombia. Renew. Energy. 2016;97:293–305.